BMB Reports - Manuscript Submission

Manuscript Draft

DOI: 10.5483/BMBRep.2022-0148

Manuscript Number: BMB-22-148

Title: Phosphorylation of rpS3 by Lyn increases translation of Multi-Drug Resistance (MDR1) gene

Article Type: Article

Keywords: RpS3; Lyn; Drug Resistance; MDR1; Ribosome Heterogeneity

Corresponding Author: Joon Kim

Authors: Woo Sung Ahn[1,#], Hag Dong Kim[2,#], Tae Sung Kim[1], Myoung Jin Kwak[1], Yong Jun Park[1], Joon Kim[1,2,*]

Institution: [1]Laboratory of Biochemistry, Division of Life Sciences, Korea University,
[2]HAEL Lab, TechnoComplex, Korea University,

Phosphorylation of rpS3 by Lyn increases translation of Multi-Drug Resistance (*MDR1*) gene

Woo Sung Ahn[1], Hag Dong Kim[2], Tae Sung Kim[1], Myoung Jin Kwak[1], Yong Jun Park[1], Joon Kim[1,2*]

[1]Laboratory of Biochemistry, Division of Life Sciences, Korea University, Seoul 02841, Republic of Korea

[2] HAEL Lab, TechnoComplex, Korea University, Seoul 02841, Republic of Korea

***Corresponding Author's Information:**

Joon Kim, Ph.D., Professor

Laboratory of Biochemistry, Division of Life Sciences, Korea University, Seoul 02841, Republic of Korea

Tel: 82-2-3290-3442, Fax: 82-2-927-9028, E-mail: joonkim@korea.ac.kr

Abstract

Lyn, a tyrosine kinase that is activated by double-stranded DNA-damaging agents, is involved in various signaling pathways, such as proliferation, apoptosis, and DNA repair. Ribosomal protein S3 (RpS3) is involved in protein biosynthesis as a component of the ribosome complex and possesses endonuclease activity to repair damaged DNA. Herein, we demonstrated that rpS3 and Lyn interact with each other, and the phosphorylation of rpS3 by Lyn, causing ribosome heterogeneity, upregulates the translation of p-glycoprotein, which is a gene product of multi-drug resistance gene 1. In addition, we found that two different regions of the rpS3 protein are associated with the SH1 and SH3 domains of Lyn. An in vitro immunocomplex kinase assay indicated that the rpS3 protein acts as a substrate for Lyn, which phosphorylates the Y167 residue of rpS3. Furthermore, by adding various kinase inhibitors, we confirmed that the phosphorylation status of rpS3 was regulated by both Lyn and doxorubicin, and the phosphorylation of rpS3 by Lyn increased drug resistance in cells by upregulating p-glycoprotein translation.

Running title: RpS3 phosphorylation increases drug resistance

Keywords: RpS3, Lyn, Drug Resistance, MDR1, Ribosome Heterogeneity

Introduction

Ribosomal protein S3 (rpS3) plays a key role in protein translation as a component of 40S ribosome. It possesses various extra-ribosomal functions, such as DNA repair (1-4), cell signaling (4-6), apoptosis/survival (7), host-pathogen interactions (8), and transcriptional regulation (9). Our previous study demonstrated that rpS3 is secreted as a homodimer in cancer cells, and the level of secretion increased as the malignancy of the tumor cells increased (10, 11). RpS3 protein and mRNA expression levels are higher in both leukemia patients and leukemia cell lines than in their normal counterparts (11, 12). These results suggest that rpS3 can be used as an indicator of tumorigenesis. Therefore, in this study, we investigated the possible role of rpS3 as a key target of anti-cancer drug resistance.

In addition to its multiple extra-ribosomal functions, rpS3 possesses several post-translational modification motifs. Although many roles of these modifications are yet to be found, several different forms of modifications have been found both *in vitro* and *in vivo*, including phosphorylation, neddylation, sumoylation, and ubiquitination, thus imparting this protein versatile functions through ribosomal heterogeneity (11). Among these, rpS3 phosphorylation has been well-studied in conjunction with its functions of DNA repair and secretion (2-4, 10, 11).

RpS3 was also identified as a mammalian DNA repair endonuclease III, which has AP endonuclease/lyase activity and is involved in base excision repair (13). In addition, rpS3 is involved in apoptosis in cases of severe DNA damage in immune cells (4). These functions are important for maintaining cellular homeostasis and are regulated through several pathways. In our previous study, we found that rpS3 exists in the promyelocytic leukemia (PML) body within the nucleus and is modified by SUMO-1 (14). Hence, rpS3 may play an important role in B-cell growth and differentiation and be associated with acute myeloid leukemia along with

PML. In this study, we investigated the correlation between post-translational modifications and signaling systems of rpS3 that can integrate control pathways, such as protein synthesis, DNA damage recovery, and cell death.

Lyn is a member of the Src family of tyrosine kinases and is predominantly expressed in hematopoietic tissues (15). Lyn plays a role in many processes, such as glutamate receptor signaling in neurons (16), cytoskeletal rearrangement and motility in mast cells, cytokine responses in hematopoietic cells (17), and B lymphocyte receptor signaling (15). This protein contains SH1 (kinase domain), SH2, and SH3 domains and a unique N-terminal sequence; the latter is dispensable for membrane localization via attachment of fatty acid myristate. The SH3 domain binds to proline-rich motifs, such as PXXP, and the SH2 domain binds to specific phosphotyrosine motifs. In addition, the SH2 and SH3 domains are involved in substrate binding and the regulation of kinase activity via intramolecular interactions (18). Studies using cell fractionation and confocal microscopy have demonstrated that Lyn kinase also exists in the nucleus (19). Nuclear Lyn, but not other Src family tyrosine kinases, are activated after genotoxic treatment, such as 1-β-$_{D}$-arabinofuranosylcytosine (Ara-C), ionizing irradiation, and adriamycin (20). Recently, BCR-ABL fusion proteins have been reported to activate Src tyrosine kinases, such as Lyn, Hck, and Fgr, to induce leukemia (21). Lyn has been studied mainly in the growth and differentiation processes of B lymphocytes (22); however, many studies have been recently conducted on its activation caused by DNA damage (23, 24). Studies on protein synthesis have revealed various regulatory mechanisms of ribosomal S6 kinase, and some studies on regulatory mechanisms for other ribosomal proteins have also been revealed (25).

P-glycoprotein (p-gp) or multidrug resistance protein (MDR1) is an adenosine triphosphate-binding cassette transporter (ABCB1) that has been intensely investigated because it is an obstacle to successful anticancer drug therapy. ABCB1 has multiple drug-binding sites, such

as etoposide, doxorubicin (DOX), paclitaxel, and vinblastine, which can bind and pump a wide variety of substrates (26). High expression levels of ABCB1 have been observed before chemotherapy in many different tumor types, including the kidney, lung, liver, colon, and rectum (27). In contrast, initially low expression and dramatically increased expression of ABCB1 after chemotherapy have been observed in many hematological malignancies, such as acute myeloid and lymphoblastic leukemia (28).

MDR, an efflux pump that transports drugs and xenobiotics out of the cell, has broad specificity. In humans, only *MDR1* can confer MDR by transfection into drug-sensitive cells (29). The antitumor drug enters the tumor cell but is quickly eliminated from the cell by the efflux action of MDR1, abolishing antitumor activity. In the uterine secretory epithelium, *MDR1* mRNA and p-gp are induced at high levels by estrogen combined with progesterone, the major steroid hormones of pregnancy (27). P-gp is post-translationally modified by differential phosphorylation and *N*-glycosylation, which are thought to affect its final functionality (30). Oncogenes such as Ras, p53, and c-Raf have been associated with the regulation of p-gp expression (31).

DOX, an anthracycline drug that intercalates DNA and inhibits DNA replication, causes the development of MDR and induces p-gp expression in several tumors (32). DOX is widely used and highly effective for the treatment of breast cancer, sarcoma, leukemia, and lymphoma (33). Inhibition of p-gp as a method to reverse MDR in patients with cancer has been studied extensively; however, the results have generally been disappointing (34).

Acute PML and chronic myeloid leukemia are associated with the activation of Src tyrosine kinases; thus, investigating the modification of the rpS3 protein could provide important insights into cancer treatment.

Herein, we found that rpS3 interacts with Lyn and that this interaction elicits the phosphorylation of rpS3. Furthermore, we investigated the effect of Lyn on rpS3

phosphorylation by adding various kinase inhibitors. We also demonstrated that the phosphorylation of rpS3 by Lyn regulates p-gp translation.

Results

RpS3 is phosphorylated after the interaction with Lyn

Our previous studies using a yeast two-hybrid system revealed that Lyn is a putative binding partner of rpS3 (14). To demonstrate the interaction of the tyrosine kinase Lyn with rpS3, we performed a co-immunoprecipitation assay using overexpression of pEGFPc1-Lyn. HEK293T cells were transfected with either a blank GFP vector or GFP vector carrying Lyn protein. As shown in Figure 1A, the interaction between rpS3 and GFP-Lyn was verified (*lane* 2); however, the interaction between rpS3 and lysate was not verified (*lane* 1). Next, we investigated whether this interaction occurs between endogenous Lyn and rpS3. We confirmed specific interactions between endogenous proteins in MPC-11 cells. Conversely, endogenous rpS3 was precipitated with antibodies against endogenous Lyn. These results indicated that rpS3 has a strong physical interaction with Lyn *in vitro* (Fig. 1A).

As Lyn is a well-known protein tyrosine kinase, we tested the possibility of rpS3 phosphorylation by Lyn. For this purpose, we performed an immunocomplex kinase assay with an anti-Lyn antibody, and recombinant His-tagged rpS3 protein was used as a substrate. Immunoprecipitates were incubated with acid-treated enolase as a positive control. As shown in Fig. 1B, autophosphorylation of Lyn demonstrated that rpS3 protein inhibits the kinase activity of Lyn. As expected, recombinant His-tagged rpS3 protein was phosphorylated by Lyn.

Collectively, these results suggest that rpS3 protein (*lane* 3) can be phosphorylated *in vitro* as much as enolase (*lane* 2), which is the positive substrate of Lyn and acts as a regulator of Lyn.

RpS3 interacts with SH3 domain of Lyn

To determine the region that is crucial for the interaction of Lyn with rpS3, a fine deletion analysis of the N- and C-termini was performed. For this purpose, we generated GST-tagged Lyn deletion constructs, as described in Fig. 2A. All the GST-tagged constructs were transferred into HEK293T cells, and GST pull-down assays were performed to target rpS3 (Fig. 2B). Furthermore, GST-tagged Lyn deletion mutants were co-transfected with a plasmid bearing GFP-tagged rpS3 into HEK293T cells, and an in vitro binding assay was performed (Fig. 2C). These results demonstrate that rpS3 binds to the SH3 domain (63–123, *lane* 3) and SH1 domain of Lyn (240–500, *lane* 5) but not to the unique N-terminal domain (1–62, *lane* 2) and SH2 domain (128–226, *lane* 4). As the binding affinity of the SH1 domain was stronger than that of SH3, we suggest that the SH1 domain of Lyn is the major binding domain with rpS3 (Fig. 2C). Furthermore, to examine the role of the SH3 domain of Lyn, we co-transfected the GFP-tagged SH3 domain of Lyn and rpS3 into Cos-1 cells (Supplementary Fig. 1). Although the wild type Lyn interacted very weakly, the SH3 domain of Lyn strongly interacted with rpS3 (*lanes* 3 and 4).

The RpS3 protein is highly basic and contains two domains: the KH domain and the S3-C terminal domain. We tested which region of rpS3 interacted with the Lyn, N-, and C-terminal deletion constructs, as described in Fig. 2D (5). Each deletion mutant was co-expressed with Lyn in HEK293T cells, and immunoprecipitation analysis was performed using cell lysates. Interestingly, rpS3 appeared to interact with Lyn *via* both N-terminal and C-terminal domains (Fig. 2E, *lanes* 5, 6, 7, 9; Open arrowheads). This result implies that there are more than one

binding sites in the rpS3. More specifically, the Lyn-binding region of rpS3 lies in the N-terminal (rpS3: 1–85, *lane* 7) and C-terminal regions (rpS3: 159–242, *lane* 3). Overall, these results suggest that the association between Lyn and rpS3 occurs by direct interaction of the Lyn SH3 domain with the C-terminal region of rpS3 (159–242, *lane* 3), or it may occur by the interaction of the Lyn SH1 domain with the N-terminal region of rpS3 (1–85, *lane* 7). The binding activity of rpS3-P (159–242, Fig. 2E, *lane* 3; GST-rpS3 C-terminal, Supplementary Fig. 2, *lane* 9) was equal to that of the wild type. These results demonstrated that the binding region of rpS3 for Lyn is within the C-terminus of the rpS3 protein. The C-terminal region (Fig. 2E, *lane* 3 and Supplementary Fig. 2, *lane* 9) contains three putative proline-rich motifs, such as PxxP, that can bind to the SH3 domain of Lyn, which raises the possibility that the SH3 domain of Lyn would take part in the interaction.

Tyrosine 167 of rpS3 is a critical residue for the phosphorylation by Lyn *in vitro*

Human rpS3 has several phosphorylation target sites, mostly serine/threonine residues (33, 34). To identify the tyrosine residue phosphorylated by Lyn, we generated a series of rpS3 mutations in which each tyrosine was substituted with phenylalanine (Fig. 3A). Subsequently, an immunocomplex kinase assay was performed (Fig. 3B). Substitution of all six tyrosine residues with phenylalanine (KS2, *lane* 4) abrogated Lyn-mediated phosphorylation. Interestingly, the double substitution mutant (KS6, *Lane* 8) also abrogated phosphorylation. Based on these results, Y166 and Y167 were assumed to be important for phosphorylation at rpS3. We generated appropriate single substitution mutants (Fig. 3C) for further investigation. The results of this analysis revealed that Y166 was weakly phosphorylated, while the Y167 residue was not phosphorylated. Therefore, we concluded that Lyn-induced rpS3 phosphorylation was eliminated by Y167F mutation of rpS3 and confirmed that the Y167 residue of rpS3 is the

critical phosphorylation site for Lyn.

We tested the effects of DOX, an anti-cancer drug that inhibits topoisomerase II, on the association of Lyn with rpS3. When GFP-rpS3 was treated with DOX, the interaction between rpS3 and Lyn increased (*Supplementary* Fig. 3, *lower panel*, *lane* 4). The results of this study suggested that DOX plays an important role in the interaction between rpS3 and Lyn.

Lyn may be activated by genotoxic agents, such as Ara-C (1-beta-D-Arabinofuranosylcytosine), adriamycin (DOX), and ionizing radiation (23). Therefore, we investigated whether the phosphorylation of rpS3 increases after treatment with genotoxins. As expected, the higher the concentration of Ara-C, the higher was the level of phosphorylated rpS3 (*Supplementary* Fig. 4, *lane* 3). However, the result may not be owing to a specific phosphorylation by Lyn; hence, we subsequently studied the effect of a global and specific inhibitor of Src family tyrosine kinases such as PP2 and genistein. Overall, rpS3 phosphorylation decreased in a dose-dependent manner. Thus, these results suggest that the phosphorylation of rpS3 is due to Src tyrosine family kinases, such as Lyn.

Increase of *MDR1* expression in DOX-resistant cells

The levels of *MDR1* mRNA and p-gp in the DOX-resistant MPC-11 cell line (MPC11-DOX) were significantly higher than that in the MPC-11 parent cells (*Supplementary* Fig. 5A). In addition, the level of tyrosine phosphorylation of rpS3 in MPC11-DOX cells increased significantly compared to that in MPC-11 parent cells (*Supplementary* Fig. 5B and 5C, *lane* 6). These results confirmed that phosphorylation of the tyrosine residue of rpS3 was increased in MPC11-DOX cells. DOX induction of p-gp expression occurred owing to the phosphorylated status of rpS3. Although a DOX-resistant cell line was established, there was little change in

the ribosome content of this cell line through the ribosomal profile, particularly in polysomes (*Supplementary* Fig. 5D). We examined the translation levels of c-Jun NH_2-Terminal kinase and rpS3 proteins in non-ribosome and ribosome fractions (35) and compared the levels of *MDR1* mRNA in parent cells (M, M') and MDR11-DOX cells (D, D') using reverse transcription polymerase chain reaction (Fig. 4A). The results demonstrated that in the ribosomal protein fractions, MDR1 mRNA was higher in MPC11-DOX cells (D, Fig. 4A, *lane* 2) than in parental cells (M, Fig. 4A, *lane* 1). MPC11-DOX cells with enhanced resistance to DOX (D', Fig 4A, *lane* 4) showed a marked increase in *MDR1* mRNA compared to the original MPC11-DOX cells (D, Fig 4A, *lane* 2). Altogether, these results suggest that selection for drug resistance, by long-term exposure to drugs, led to the establishment of a boosted DOX-resistant cell line D', in which the translational block of *MDR1* mRNA was overcome such that the mRNA was translated and p-gp was overexpressed (36). Based on these results (Fig. 3C), we performed in vivo quantitative measurements of p-gp synthesis following control rpS3-WT or Y166D and Y167D as substrates (phosphomimetic form) in MPC11-DOX cells using [S^{35}]-methionine labeling (Fig. 4B). P-gp of Y166D (*lane* 3) was similar to that of the wild type. In the case of Y167D (*lane* 4), p-gp expression level was three-fold higher than that of the wild type (*lane* 2). This suggests that protein synthesis (i.e., translation) of p-gp is upregulated by the phosphorylation of rpS3 by Lyn.

Discussion

RpS3 is an essential constituent of the 40S subunit of the ribosome and is involved in protein translation. However, the extra-ribosomal functions of many ribosomal proteins have not yet

been elucidated. RpS3 has been extensively studied for its functions outside of the translational machinery, and multiple roles in DNA damage repair and apoptosis have been reported (1, 4, 11).

Overexpression of rpS3 in colorectal cancers has been reported, and the relationship between rpS3 and cancer development has long been suspected. In this regard, we studied the relationship between leukemia-related carcinogenesis and the modification of rpS3. Based on the regulatory properties of Lyn in tumorigenesis and its biochemical relationships with various binding partners, we hypothesized that the relationship between rpS3 and Lyn could be functionally involved in the drug resistance of MPC11 cells. The antitumor effect of DOX primarily involves topoisomerase-mediated double-strand DNA breaks with the subsequent triggering of DNA damage-associated cell cycle arrest and apoptosis pathways. In this study, we showed the interaction between the rpS3 protein and Lyn, demonstrating the phosphorylation of rpS3 by Lyn (Fig. 1). The SH3 domain of Lyn contains a module that can bind to the proline-rich motif (PxxP) (25-27). Although three putative proline-rich motifs that lie in the C-terminus of rpS3 are not exactly matched with the conserved proline-rich motifs, our results showed that the putative proline-rich motifs of rpS3 interacted with the SH3 domain of Lyn (Fig. 2C). However, to identify the binding sites between the rpS3 and SH3 domains of Lyn, further studies need to be carried out, such as point mutations in three putative proline-rich motifs. Furthermore, we showed that the SH1 domain of Lyn interacted with rpS3 (Fig. 2C).

The results of kinase assay also revealed that rpS3 is directly phosphorylated by Lyn, and the level of phosphorylation is comparable to that for enolase, a typical phosphorylation target of Lyn (Fig. 1B). In addition, we demonstrated that rpS3 inhibits the autophosphorylation of Lyn. Collectively, our data demonstrated that rpS3 is a substrate of Lyn kinase. Lyn phosphorylates

166Y and 167Y in rpS3 (Fig. 3C), and Y167 is a critical residue for rpS3 function.

Lyn is activated by various agents that arrest DNA replication or damage (20, 35). Herein, we demonstrated that the phosphorylation of rpS3 was increased by treatment with genotoxic agents and decreased by the addition of a specific inhibitor of Src family tyrosine kinases, such as PP2 (*Supplementary* Fig. 4). In addition, we showed that phosphorylation was completely abolished by the addition of general tyrosine kinase inhibitors, such as genistein.

Although further studies are needed to clarify the precise role of Lyn phosphorylation on rpS3, we suggest that phosphorylation may affect the repair activity of rpS3.

RpS3 is subjected to various post-translational modifications, such as phosphorylation, sumoylation, methylation, and ubiquitination (3, 5, 11, 13, 37, 38). These modifications also lead to ribosome heterogeneity, resulting in differential translational products (39).

Various modifications and changes in the expression level of the rpS3 protein occur when cells are under various types of stress. We confirmed that phosphorylation of the tyrosine residue of rpS3 was increased in response to genotoxic stress, and p-gp, with the phospho-mimic form of Y167D, was higher than that of the wild type (Fig. 4B). This suggests that p-gp protein synthesis is regulated by the phosphorylation of rpS3 by Lyn *via* ribosome heterogeneity.

In conclusion, our study identified the interaction between Lyn and rpS3 and the phosphorylation of rpS3 by activated Lyn. This phosphorylation of rpS3 by Lyn increased the translation of p-gp, a gene product of *MDR1* (multi-drug resistance gene 1). This phosphorylation of rpS3 by Lyn may result in increased drug resistance in cancer cells.

Materials and methods

Further detailed information is provided in the *Supplementary* Information.

Acknowledgements

This study was supported in part by NRF-2020R1A2C2100803 and NRF-2021R1A6A1A10045235.

References

1. Kim J, Chubatsu LS, Admon A, Stahl J, Fellous R and Linn S (1995) Implication of mammalian ribosomal protein S3 in the processing of DNA damage. J Biol Chem 270, 13620-13629
2. Kim SH, Lee JY and Kim J (2005) Characterization of a wide range base-damage-endonuclease activity of mammalian rpS3. Biochem Biophys Res Commun 328, 962-967
3. Kim TS, Kim HD and Kim J (2009) PKCdelta-dependent functional switch of rpS3 between translation and DNA repair. Biochim Biophys Acta 1793, 395-405
4. Jang CY, Lee JY and Kim J (2004) RpS3, a DNA repair endonuclease and ribosomal protein, is involved in apoptosis. FEBS Lett 560, 81-85
5. Kim TS, Jang CY, Kim HD, Lee JY, Ahn BY and Kim J (2006) Interaction of Hsp90 with ribosomal proteins protects from ubiquitination and proteasome-dependent degradation. Mol Biol Cell 17, 824-833
6. Kim HD, Kim TS and Kim J (2011) Aberrant ribosome biogenesis activates c-Myc and ASK1 pathways resulting in p53-dependent G1 arrest. Oncogene 30, 3317-3327
7. Sen N, Paul BD, Gadalla MM et al (2012) Hydrogen sulfide-linked sulfhydration of NF-κB mediates its antiapoptotic actions. Mol Cell 45, 13-24
8. Gao X, Wan F, Mateo K et al (2009) Bacterial effector binding to ribosomal protein s3 subverts NF-kappaB function. PLoS Pathog 5, e1000708
9. Wan F, Anderson DE, Barnitz RA et al (2007) Ribosomal protein S3: a KH domain subunit in NF-kappaB complexes that mediates selective gene regulation. Cell 131, 927-939
10. Kim Y, Kim HD, Youn B, Park YG and Kim J (2013) Ribosomal protein S3 is secreted as a homodimer in cancer cells. Biochem Biophys Res Commun 441, 805-808
11. Kim Y, Lee MS, Kim HD and Kim J (2016) Ribosomal protein S3 (rpS3) secreted from various cancer cells is N-linked glycosylated. Oncotarget 7, 80350-80362
12. Hua W, Yue L and Dingbo S (2016) Over-Expression of RPS3 Promotes Acute Lymphoblastic Leukemia Growth and Progress By Down-Regulating COX-2 through NF-κb Pathway. Blood 128, 3927
13. Park YJ, Kim SH, Kim TS et al (2021) Ribosomal protein S3 associates with the TFIIH complex and positively regulates nucleotide excision repair. Cell Mol Life Sci 78, 3591-3606
14. Jang CY, Shin HS, Kim HD, Kim JW, Choi SY and Kim J (2011) Ribosomal protein S3 is stabilized by sumoylation. Biochem Biophys Res Commun 414, 523-527
15. Yamanashi Y, Kakiuchi T, Mizuguchi J, Yamamoto T and Toyoshima K (1991) Association of B cell antigen receptor with protein tyrosine kinase Lyn. Science 251, 192-194
16. Hayashi T, Umemori H, Mishina M and Yamamoto T (1999) The AMPA receptor interacts with and signals through the protein tyrosine kinase Lyn. Nature 397, 72-76
17. Suzuki T, Shoji S, Yamamoto K et al (1998) Essential roles of Lyn in fibronectin-mediated filamentous actin assembly and cell motility in mast cells. J Immunol 161, 3694-3701
18. Grishin A, Sinha S, Roginskaya V et al (2000) Involvement of Shc and Cbl-PI 3-kinase in Lyn-

dependent proliferative signaling pathways for G-CSF. Oncogene 19, 97-105

19. Corey SJ, Dombrosky-Ferlan PM, Zuo S et al (1998) Requirement of Src kinase Lyn for induction of DNA synthesis by granulocyte colony-stimulating factor. J Biol Chem 273, 3230-3235
20. Mayer BJ (2001) SH3 domains: complexity in moderation. J Cell Sci 114, 1253-1263
21. Kharbanda S, Saleem A, Yuan ZM et al (1996) Nuclear signaling induced by ionizing radiation involves colocalization of the activated p56/p53lyn tyrosine kinase with p34cdc2. Cancer Res 56, 3617-3621
22. DeFranco AL, Chan VW and Lowell CA (1998) Positive and negative roles of the tyrosine kinase Lyn in B cell function. Semin Immunol 10, 299-307
23. Yoshida K, Weichselbaum R, Kharbanda S and Kufe D (2000) Role for Lyn tyrosine kinase as a regulator of stress-activated protein kinase activity in response to DNA damage. Mol Cell Biol 20, 5370-5380
24. Yoshida K, Kharbanda S and Kufe D (1999) Functional interaction between SHPTP1 and the Lyn tyrosine kinase in the apoptotic response to DNA damage. J Biol Chem 274, 34663-34668
25. Hu Y, Liu Y, Pelletier S et al (2004) Requirement of Src kinases Lyn, Hck and Fgr for BCR-ABL1-induced B-lymphoblastic leukemia but not chronic myeloid leukemia. Nat Genet 36, 453-461
26. Satake K, Tsukamoto M, Mitani Y et al (2015) Human ABCB1 confers cells resistance to cytotoxic guanidine alkaloids from Pterogyne nitens. Biomed Mater Eng 25, 249-256
27. Fojo AT, Ueda K, Slamon DJ, Poplack DG, Gottesman MM and Pastan I (1987) Expression of a multidrug-resistance gene in human tumors and tissues. Proc Natl Acad Sci U S A 84, 265-269
28. Baudis M, Prima V, Tung YH and Hunger SP (2006) ABCB1 over-expression and drug-efflux in acute lymphoblastic leukemia cell lines with t(17;19) and E2A-HLF expression. Pediatr Blood Cancer 47, 757-764
29. Arceci RJ, Baas F, Raponi R, Horwitz SB, Housman D and Croop JM (1990) Multidrug resistance gene expression is controlled by steroid hormones in the secretory epithelium of the uterus. Mol Reprod Dev 25, 101-109
30. Lelong-Rebel IH and Cardarelli CO (2005) Differential phosphorylation patterns of P-glycoprotein reconstituted into a proteoliposome system: insight into additional unconventional phosphorylation sites. Anticancer Res 25, 3925-3935
31. Chen KG and Sikic BI (2012) Molecular pathways: regulation and therapeutic implications of multidrug resistance. Clin Cancer Res 18, 1863-1869
32. Kuo MT (2009) Redox regulation of multidrug resistance in cancer chemotherapy: molecular mechanisms and therapeutic opportunities. Antioxid Redox Signal 11, 99-133
33. Meredith AM and Dass CR (2016) Increasing role of the cancer chemotherapeutic doxorubicin in cellular metabolism. J Pharm Pharmacol 68, 729-741

34. Thomas H and Coley HM (2003) Overcoming multidrug resistance in cancer: an update on the clinical strategy of inhibiting p-glycoprotein. Cancer Control 10, 159-165
35. Kim TS, Kim HD, Park YJ et al (2019) JNK activation induced by ribotoxic stress is initiated from 80S monosomes but not polysomes. BMB Rep 52, 502-507
36. Beausoleil SA, Villen J, Gerber SA, Rush J and Gygi SP (2006) A probability-based approach for high-throughput protein phosphorylation analysis and site localization. Nat Biotechnol 24, 1285-1292
37. Shin HS, Jang CY, Kim HD, Kim TS, Kim S and Kim J (2009) Arginine methylation of ribosomal protein S3 affects ribosome assembly. Biochem Biophys Res Commun 385, 273-278
38. Jung Y, Kim HD, Yang HW, Kim HJ, Jang CY and Kim J (2017) Modulating cellular balance of Rps3 mono-ubiquitination by both Hel2 E3 ligase and Ubp3 deubiquitinase regulates protein quality control. Exp Mol Med 49, e390
39. Yang HW, Kim HD, Kim TS and Kim J (2019) Senescent Cells Differentially Translate Senescence-Related mRNAs Via Ribosome Heterogeneity. J Gerontol A Biol Sci Med Sci 74, 1015-1024

Figure legends

Figure 1. RpS3 interacts with Lyn in vitro.

(A) HEK293T cells were transfected with pEGFPc1 or pEGFPc1-Lyn plasmids. Cell extracts were immunoprecipitated (IP) using anti-Lyn antibody, and immunprecipitated proteins were resolved by 10% SDS-PAGE and immunoblotted (IB) using the indicated antibody. Ig(H); heavy chain, Ig(L); Light chain. **(B)** Lyn interacts with and phosphorylates rpS3. MPC-11 cell lysates were immunoprecipitated with Lyn antibody, and an *in vitro* kinase assay was performed using purified His-rpS3. Proteins were analyzed by 10% SDS-PAGE and subsequent autoradiography. Enolase was used as a positive control. Asterisk indicates Lyn autophosphorylation. Phosphorylation was detected by isotope labeling with γ-^{32}P ATP followed by phosphor imaging analysis. The data represent three independent experiments.

Figure 2. Identification of interaction domain of rpS3 with Lyn.

(A) Schematic representation of GST-Lyn deletion constructs. **(B)** HEK293T cells were cotransfected with pEBG-Lyn deletion mutants and pEGFP-rpS3. Immunoblotting assay of the different GST-Lyn deletion mutants. GST and GST-Lyn fusion proteins (WT or deletion mutant, *lower panel*). Bacterial lysates containing each protein were prepared as described in Materials and Methods and incubated with glutathione-agarose. The glutathione agarose was then washed, and bound proteins were eluted with 20 mM free glutathione. The purified GST (*lane* 1), GST-Lyn unique domain (*lane* 2), GST-Lyn SH3 (*lane* 3), GST-Lyn SH2 (*lane* 4), GST-Lyn kinase domain (*lane* 5), and GST-Lyn wild type (*lane* 6) fusion proteins were resolved by electrophoresis on an 10% SDS-PAGE and visualized by immunoblotting assay with GFP and GST antibodies. **(C)** Lyn domain interacted with rpS3 using by immunoprecipitation (*upper*

panel) and co-immunoprecipitation (*lower panel*) assay. Cell extracts were immunoprecipitated (IP) using anti-GFP antibody, and immunprecipitated proteins were resolved by 10% SDS-PAGE and immunoblotted (IB) using the indicated antibody. Ig(H), heavy chain, Ig(L), Light chain. Asterisks indicate GST-K domain (*lower panel*, *lane* 5). **(D)** Schematic representation of GST-rpS3 deletion constructs. The numbers indicate amino acid (a.a) positions in rpS3. (**E)** HEK293T cells were cotransfected with pEBG-rpS3 deletion mutants and pcDNA3-Lyn. After 24 h, cells were lysed, and extracts were pulled down with glutathione-Sepharose beads. Isolated GST fusion proteins were resolved by 10% SDS-PAGE and immunoblotted with Lyn (*upper panel*) and GST (*middle panel*) antibodies. *Open arrowheads* indicate the positions of GST and GST-rpS3 constructs and GST, respectively. WT, wild type. Y, Tyrosine. RpS3 deletion mutants interacted with Lyn by immunoprecipitation assay (*lower panel*). Cell extracts were immunoprecipitated (IP) using anti-Lyn antibody, and immunprecipitated proteins were resolved by 10% SDS-PAGE and immunoblotted (IB) using the indicated antibody. Ig(H), heavy chain, Ig(L), Light chain. *Open arrowheads* indicate the interaction positions of pEBG-rpS3 deletion mutants with pcDNA3-Lyn, respectively. The data represent three independent experiments.

Figure 3. RpS3 phosphorylates Lyn at Y167.

(A) Schematic representation of GST-rpS3 point mutation (Tyr→Phe) constructs. The numbers indicate tyrosine positions in rpS3. **(B)** MPC-11 cell lysates were immunoprecipitated with Lyn antibody, and an in vitro kinase assay was performed using purified pET21a-rpS3. Proteins were analyzed by 10% SDS-PAGE and subsequent Coomassie blue staining (*upper panel*) and autoradiography (*lower panel*). Enolase was used as a positive control. Asterisks indicate Lyn

autophosphorylation. **(C)** MPC-11 cell lysates were immunoprecipitated with Lyn antibody, and an *in vitro* kinase assay was performed using purified His-rpS3 Y166 and Y167. Proteins were analyzed by 10% SDS-PAGE and subsequent autoradiography. Enolase was used as a positive control. Asterisk indicates Lyn autophosphorylation. **(D)** schematic representation of GST-rpS3 deletion constructs. The numbers indicate amino acid (a.a) positions in rpS3. **(E)** HEK293T cells were cotransfected with pEBG-rpS3 deletion mutants and pcDNA3-Lyn. After 24 h, cells were lysed, and extracts were pulled down with glutathione-Sepharose beads. Isolated GST fusion proteins were resolved by 10% SDS-PAGE and immunoblotted with Lyn (*upper panel*) and GST (*middle panel*) antibodies. Open arrowheads indicate the positions of GST and GST-rpS3 constructs, respectively. WT, wild type. Y, Tyrosine. RpS3 deletion mutants interacted with Lyn by immunoprecipitation assay (*lower panel*). *Open arrowheads* indicate the positions of GST and GST-rpS3 constructs, respectively. Cell extracts were immunoprecipitated (IP) using anti-Lyn antibody, and immunprecipitated proteins were resolved by 10% Sodium Dodecyl Sulfate-PolyAcrylamide Gel Electrophoresis (SDS-PAGE) and immunoblotted (IB) using the indicated antibody. Ig(H), heavy chain, Ig(L), Light chain. *Open arrowheads* indicate the interaction positions of pEBG-rpS3 deletion mutants with pcDNA3-Lyn, respectively. The data represent three independent experiments.

Figure 4. Identification of activity translated *MDR1* mRNA.

(A) Non-ribosomal and ribosomal protein were fractionated. Both fractions were immunoblotted with JNK and rpS3 antibodies. *MDR1* and *GAPDH* transcripts from the cells were amplified by RT-PCR and detected by Southern blot hybridization using oligonucleotide probes. GAPDH was used as an internal control. **(B)** S^{35}-Methione labeling was used to investigate *in vivo* quantitative measurements of p-glycoprotein synthesis of Y166D and Y167D

(a phosphorylation-mimetic mutant) in MPC11-DOX cells. Equal amounts of proteins were resolved by 10% SDS-PAGE and analyzed by autoradiography. Control FL (Flag), wild type rpS3 (W) and Y166D, Y167D; Tyrosine to aspartic acid substituted mutants. Tubulin antibody was used as an internal control. The data represent three independent experiments.

Figure 1

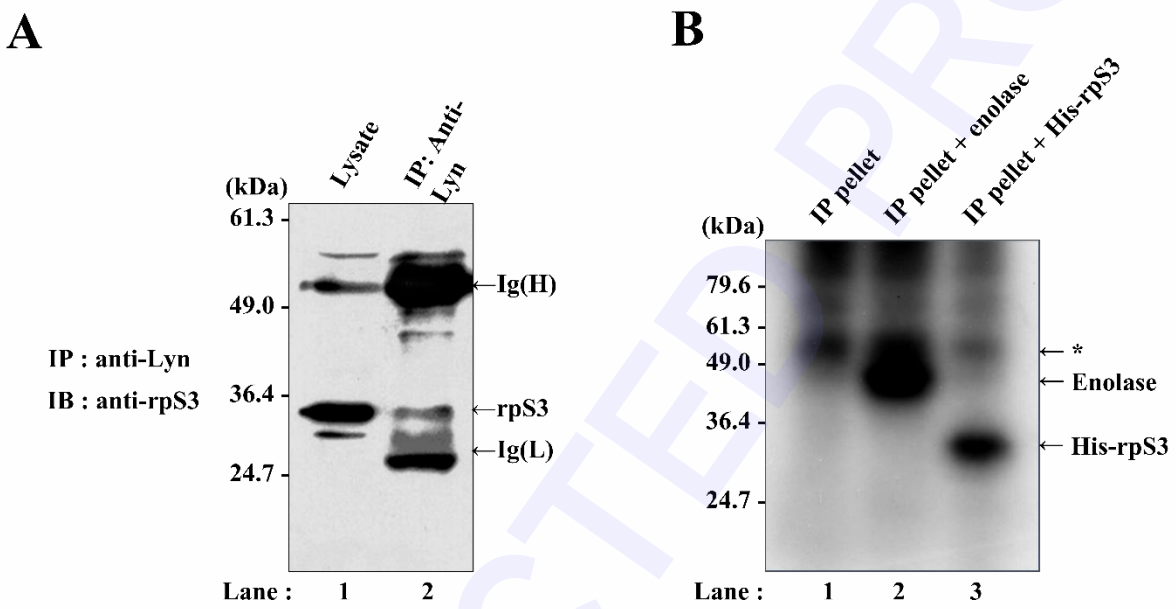

Figure 2

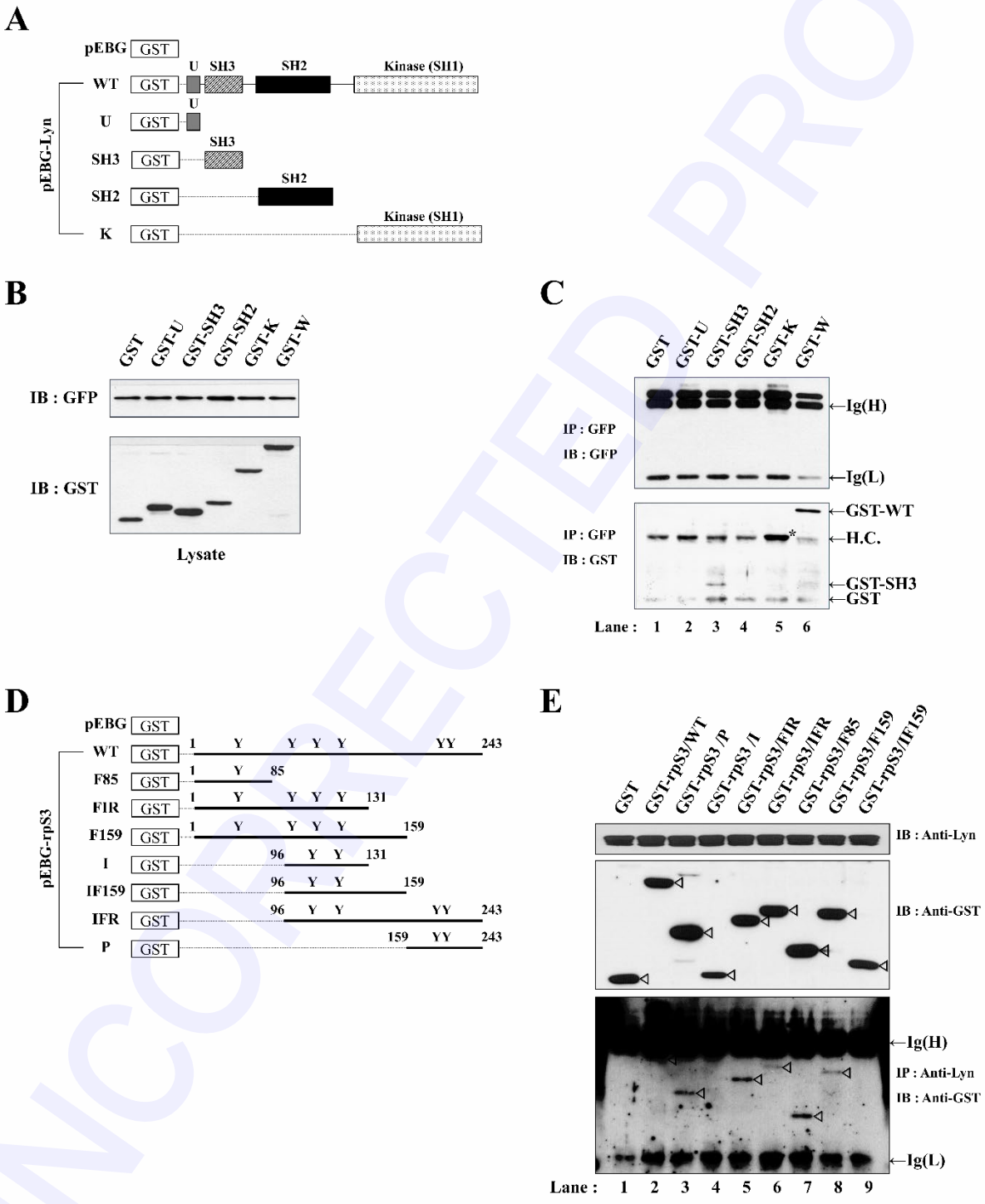

Figure 3

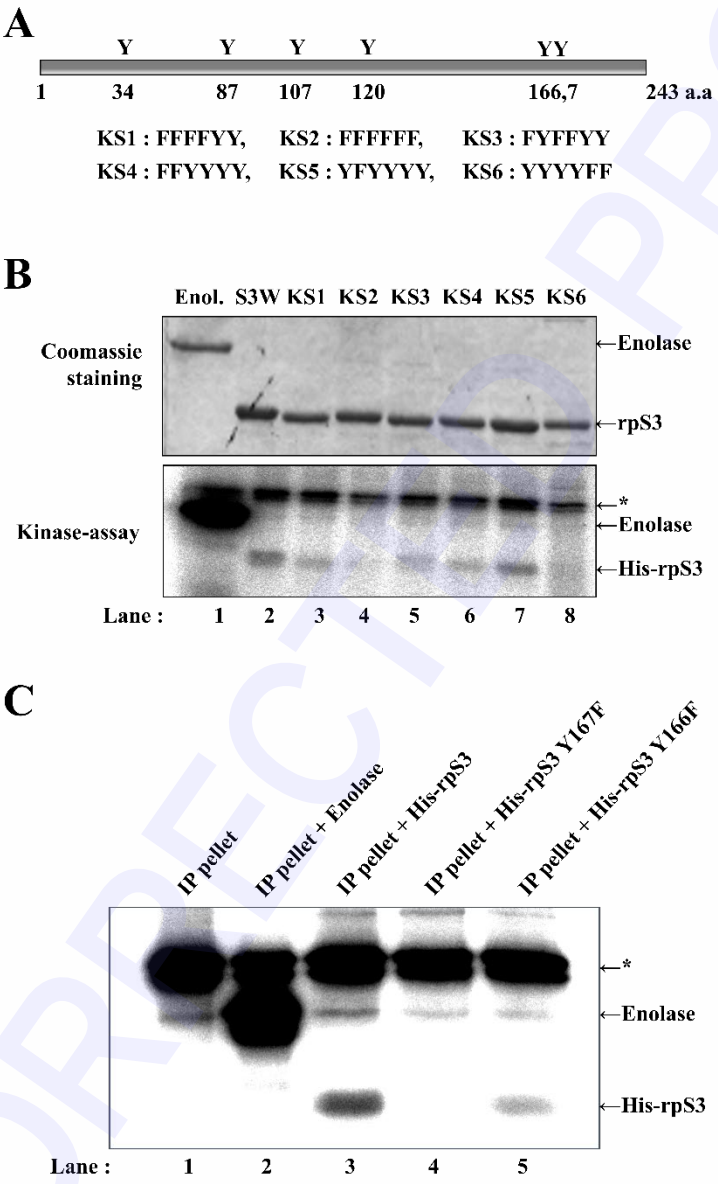

Figure 4

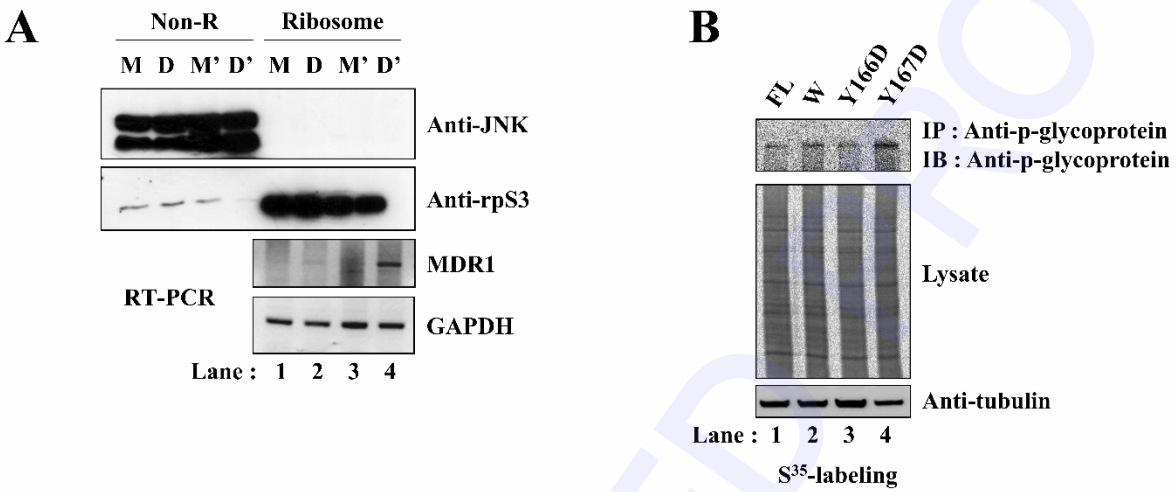

Manuscript Type: Article

Title: *Phosphorylation of rpS3 by Lyn increases translation of Multi-Drug Resistance gene (MDR1)*

Supplementary File

Author's name: Woo Sung Ahn[1], Hag Dong Kim[2], Tae Sung Kim[1], Myoung Jin Kwak[1], Yong Jun Park[1], Joon Kim[1,2*]

Affiliation:

[1]Laboratory of Biochemistry, Division of Life Sciences, Korea University, Seoul 02841, Republic of Korea

[2] HAEL Lab, TechnoComplex, Korea University, Seoul 02841, Republic of Korea

Running title: RpS3 phosphorylation increases drug resistance

Keywords: RpS3, Lyn, Drug Resistance, MDR1, Ribosome Heterogeneity

***Corresponding Author's Information:**

Joon Kim, Ph.D., Professor

Laboratory of Biochemistry, Division of Life Sciences, Korea University, Seoul 02841, Republic of Korea.

Tel: 82-2-3290-3442, Fax: 82-2-927-9028, E-mail: joonkim@korea.ac.kr

Supporting information materials and methods

Antibodies and reagents

Monoclonal β-actin, GFP, phospho-Tyr, anti-GFP, polyclonal anti-Lyn, anti-GST, and p-glycoprotein antibodies were obtained from Santa Cruz Biotechnology Inc. (Santa Cruz, CA, USA), and monoclonal anti-FLAG and anti-tubulin antibodies were obtained from Sigma-Aldrich Co. (St. Louis, MO, USA). Phospho-tyrosine antibody was obtained from BD Transduction Laboratories (San Jose, CA, USA), and rabbit polyclonal RPS3 antibody was obtained from HAEL (Korea University, Seoul, Korea). Horseradish peroxidase (HRP)-conjugated goat anti-rabbit IgG and goat anti-mouse IgG secondary antibodies were purchased from Jackson ImmunoResearch (West Grove, PA, USA). Enhanced chemiluminescence (ECL) reagents were purchased from Roche (Mannheim, Germany), and protein A-Sepharose was purchased from Roche Applied Science. Adriamycin (doxorubicin [DOX]) was obtained from Upstate Biotechnology, Inc. (Lake Placid, NY, USA). Ara-C (cytosine arabinoside, 1-β-D-arabinofuranosylcytosine, cytarabine), genistein (5, 7, 4′-trihydroxyisoflavone), and dimethyl sulfoxide (DMSO) were purchased from Sigma Chemical Co. (St. Louis, MO, USA), and glutathione-Sepharose 4 B was purchased from Amersham Biosciences (Piscataway, NJ, USA).

Plasmids

The full-length human rpS3 gene was cloned in-frame with a sequence coding for FLAG (pcDNA3-Flag, Invitrogen, Carlsbad, CA, USA), EGFP (pEGFPc1, BD Biosciences Clontech, Palo Alto, CA, USA), His (pET21a, Novagen, Germany), and glutathione S-transferase (GST, pEBG, Amersham Biosciences, NJ, USA). Human *rpS3* deletion mutant sequences were amplified by polymerase chain reaction (PCR), using eight primer pairs. The resulting PCR

products were cut with *EcoRI* and *XhoI* and cloned in-frame into the pGEX5x-1. GST *rpS3* deletion mutants were generated, expressed, and purified as previously described (1). Full-length human *lyn* gene was cloned into pCDNA3 (pcDNA3-Flag, Invitrogen, Carlsbad, CA, USA).

Site-directed mutagenesis

Site-directed mutagenesis was performed by overlap extension using PCR. The *rpS3* gene cloned into the pGEM-T Easy vector (Promega, Madison, WI, USA) was used as a template for mutagenesis. Two sets of PCR reactions were carried out. The first PCR fragment was synthesized using the *rpS3*-forward primer and an antisense mutagenic primer. The second PCR fragment was synthesized using the *rpS3*-reverse primer and a sense mutagenic primer. The two amplified products were mixed, annealed, and polymerized using Taq polymerase (Takara, Otsu, Shiga, Japan). Using this product as a template, PCR was performed by employing the rpS3-forward and -reverse primers.

Protein expression and purification

Escherichia coli strain BL21(DE3)/pLysS (Novagen, Germany) cells were transformed with pET21a and pGEX5x-1 based plasmids. The transformed cells were grown in Luria–Bertani (LB) broth containing 50 μg/mL ampicillin at 37 ºC overnight, and one hundredth of the cells were then grown in the LB broth containing 50 μg/mL ampicillin, 0.4% dextrose at 30 ºC until the cell density reached A_{600} = 0.6–0.8. The recombinant proteins were expressed after induction with 0.5 mM isopropyl-1-β-D-galactopyranoside and purified with glutathione-Sepharose 4 B (Amersham Biosciences, NJ, USA) and Ni^{2+}-NTA beads (Qiagen, Valencia, CA, USA), according to the manufacturer's instructions.

Cell culture and Transfections

Human embryonic kidney epithelial 293T and mouse plasmacytoma MPC11 cells were grown in Dulbecco's modified Eagle's medium (DMEM; WelGENE Inc., Korea) supplemented with 10% heat-inactivated fetal bovine serum (FBS; WelGENE Inc., Korea), 100 U/mL penicillin, 100 μg/mL streptomycin, and 2 mM L-glutamine. The cells were maintained at 37 ºC in a humidified atmosphere containing 5% CO_2. HEK293 cells were seeded in 6-well plates at a density of 1 × 10^6 cells per well and incubated for 24 h before the experiment. Transfections were performed using Lipofectamine (Invitrogen, Carlsbad, CA, USA), according to the manufacturer's instructions.

Cell culture of doxorubicin-resistant MPC11 cell line (MPC11-DOX)

Mouse plasmacytoma MPC-11 cells were maintained in DMEM (WelGENE Inc., Korea) supplemented with 10% FBS (WelGENE Inc., Korea) and grown at 37 °C in a humidified atmosphere of 5% CO_2. MPC-11 cells were cultured in serially increasing concentrations of DOX for 45 d to establish the MPC11-DOX cell line. The MPC11-DOX cell line was cultured in DOX-free medium before experiments (2).

Ribosome Fractionation

MPC11-DOX cells were treated with the indicated drugs, and ribosome fractionation and immunoprecipitation were performed as previously described (3).

Reverse Transcription Polymerase Chain Reaction (RT-PCR)

Cells were harvested after treatment (described above), and total RNA was isolated for RT-PCR analysis using a previously described method (4). Primers for *MDR1*, *rpS3*, *rpS5,* and

glyceraldehyde 3-phosphate dehydrogenase (*GAPDH)* were designed using Primer Express 4.0 (Applied Biosystems, Foster, CA, USA). For the RT-PCR control, total RNA from MPC-11 cells (5×10^5 cells) was extracted with TRIzol reagent (Invitrogen, Carlsbad, CA, USA). RNAs were reverse transcribed using oligo(dT)-15. The PCR products were visualized on 1% TAE-agarose gel. RT-PCR was performed using a LightCycler® 96 Real-Time PCR System (Roche, Basel, Switzerland) as follows: initial denaturation at 94 °C for 5 min, followed by 30 cycles of 94 °C for 30 s, 56 °C for 30 s, and 72 °C for 40 s, and final elongation at 72 °C for 10 min. The intensity of each gene was normalized to that of (GAPDH). The primers used for PCR are as follows: 5′-CCC ATC ATT GCA ATA GCA GG-3′ (forward), 5′-TGT TCA AAC TTC TGC TCC TGA-3′ (reverse) of the *MDR1* gene, 5′-AGC GGA GAC CCT GTT AAC TAC TAC-3′ (forward), 5′-GTC TTT CTA CAA AAT TTT ATT AAA GG-3′ (reverse) of the *rpS3* gene (5), 5′-GAA GGT GAA GGT CGG AGT C-3′ (forward), and 5′-GAA GAT GGT GAT GGG ATT TC-3′ (reverse) of the *GAPDH* gene. The *MDR1* and *GAPDH* primers yielded products of 158 and 226 bp, respectively.

In vitro binding assay

GST fusion proteins were purified using glutathione-sepharose 4B beads. *In vitro* binding assays were performed by incubating immobilized GST fusion proteins with HEK293T cell lysates of desired protein expressed at 4 ºC for 16 h. After extensive washing, the protein-protein complex was boiled in sodium dodecyl sulfate-polyacrylamide gel electrophoresis (SDS-PAGE) sample buffer, separated by SDS-PAGE, and transferred to nitrocellulose membranes.

Immunoblot assay

Cells were harvested and lysed on ice in TNN lysis buffer (20 mM Tris-HCl [pH 7.5], 150 mM

NaCl, 50 mM NaF, 1 mM Na_3VO_4) in the presence of protease inhibitors (2 mM phenylmethylsulfonyl fluoride (PMSF), 1 µg/mL aprotinin, 1 µg/mL leupeptin, and 1 µg/mL pepstatin A) for 30 min on ice. Supernatants were collected by centrifugation at 12,000 × g for 10 min at 4 ºC, and protein concentration was determined by the Bradford protein assay. The lysates were boiled in SDS-PAGE sample buffer, separated by SDS-PAGE, and transferred to polyvinylidene difluoride membranes (Millipore, Schwalbach, Germany). Membranes were blocked with 5% nonfat dry milk for 1 h. Blots were incubated with primary antibody in blocking solution for 1 h at 4 °C. Membranes were rinsed twice with Tris-buffered saline, 0.1% Tween 20 and incubated with HRP-conjugated secondary antibody (1:2000) (Chemicon International, Temecula, CA, USA) in blocking solution for 30 min. The cells were illuminated with an ECL system (Roche Applied Science, Mannheim, Germany) and detected using a BAS2500 imaging analyzer (Fujifilm, Tokyo, Japan). Antibodies against actin (Millipore) were used to normalize the sample loading.

Immunoprecipitation

Transfected HEK293T cells were lysed using cold TNN lysis buffer (50 mM Tris-HCl [pH 7.5], 150 mM NaCl, 1% NP-40, and 0.5% sodium deoxycholate) in the presence of protease inhibitors (2 mM PMSF, 1 µg/mL aprotinin, and 1 µg/mL leupeptin) for 30 min on ice. After centrifugation at 12,000 ×g for 10 min at 4 ºC, supernatant was collected. The supernatant was precleared by adding protein A agarose and was then incubated at 4 ºC for 2 h with the desired antibody. Clarified lysates were incubated with 1–2 g of the appropriate antibody for 2 h, followed by 25 µL of a 50% slurry of protein A-agarose (Roche Applied Science, Mannheim, Germany) for 3–16 h at 4 °C. After extensive washing, immunoprecipitants were resuspended in SDS-PAGE sample buffer and separated by SDS-PAGE.

In vitro Kinase assay

The cell lysates were subjected to immunoprecipitation using an anti-Lyn antibody. The immunoprecipitates were washed thrice with lysis buffer, twice with tyrosine kinase buffer (50 mM HEPES [pH 7.4], 10 mM $MnCl_2$, 10 mM $MgCl_2$, 2 mM DTT, and 0.1 mM Sodium vanadate). The reaction mixture was initiated by the addition of 2.0 µCi of [γ-^{32} P] ATP and 5 µg of *E.coli* purified His-rpS3 or 5 µg of acid-treated enolase substrate and incubated at 30 °C. After 30 min of incubation, the reaction was stopped by the addition of 20 µL of 2 × SDS-sample buffer (100mM Tris-HCl [pH 6.8], 2% 2-Mercaptoethanol, 4% SDS, 20% glycerol, and 0.04% bromophenol blue) and subjected to 10% SDS-PAGE. After the gel was dried, phosphorylated protein was visualized using a BAS2500 imaging analyzer (Fujifilm, Tokyo, Japan).

Drugs and preparation of pervanadate

Adriamycin (DOX) was obtained from Upstate Biotechnology, Inc. (Lake Placid, NY, USA). PP2 and genistein were obtained from Calbiochem (EMD Millipore, Billerica, MA, USA) and dissolved in DMSO. Sodium pervanadate was prepared as a 50 mM stock solution using the following procedure. Sodium orthovanadate (2 mL of 100 mM; Sigma, St. Louis, MO, USA) solution was activated by mixing with 2 mL of 100 mM hydrogen peroxide solution, and the reaction was allowed to proceed for 15 min at room temperature (26 ± 2°C). The reaction was terminated by the addition of 400 U/mL of catalase (15 min) to remove residual H_2O_2, after which the pervanadate solution was ready for use.

Statistical analysis

Statistical significance was determined using the Student's t-test. Differences were considered

significant if the p-value was <0.05(*) or 0.01(**). Each error bar represents standard deviation.

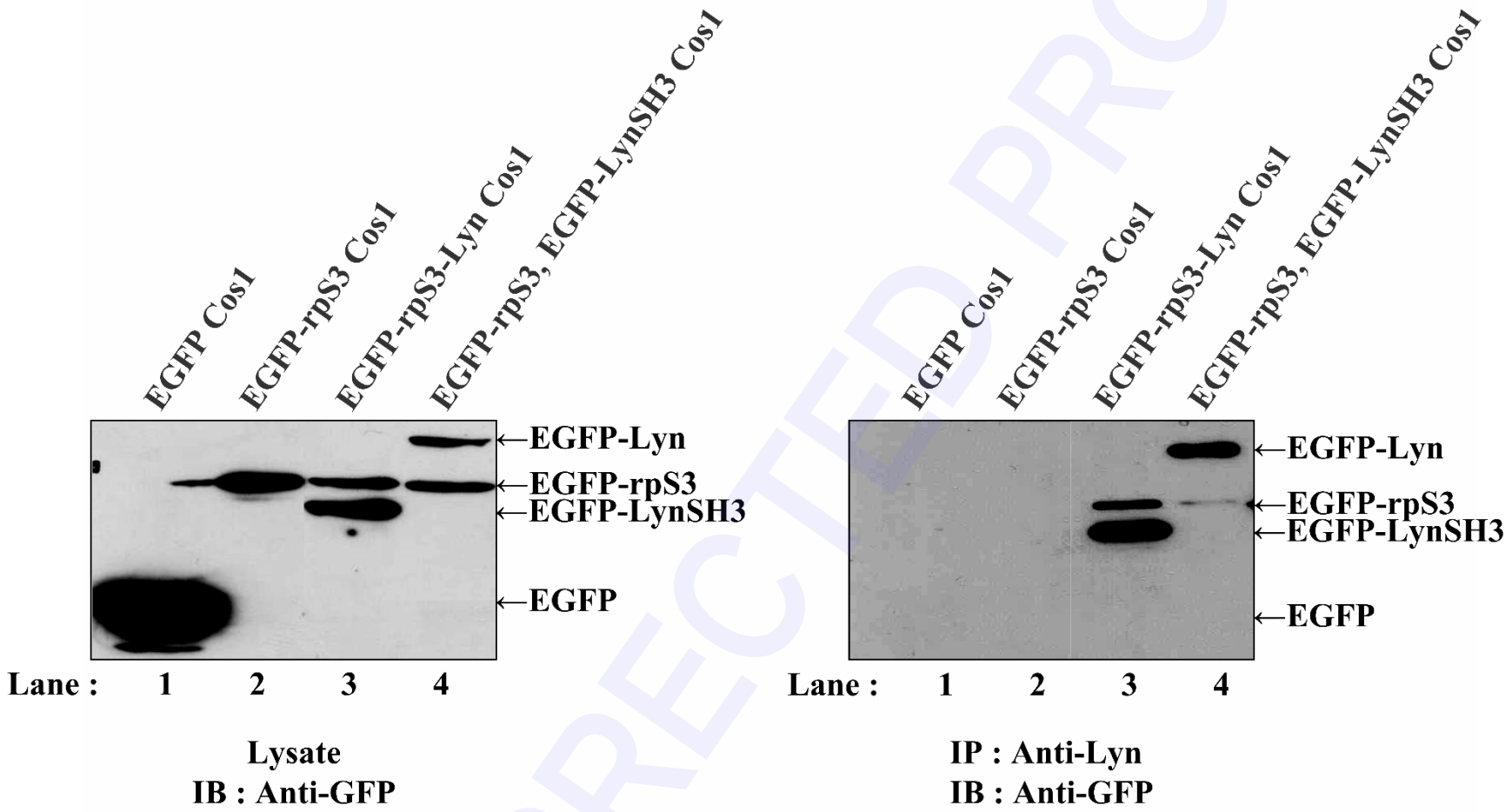

Supplementary Figure 1. Ribosomal protein S3 (rpS3) interacts with Src homology 3 (SH3) domain of Lyn

Cos-1 cells were transiently transfected with GFP-rpS3 plus GFP-Lyn or GFP-rpS3 plus GFP-LynSH3. Lysates were subjected to immunoprecipitation with anti-Lyn antibody. Co-immunoprecipitants and cell lysates were separated by 10% Sodium Dodecyl Sulfate -

PolyAcrylamide Gel Electrophoresis (SDS-PAGE) and analyzed by immunoblotting with anti-GFP antibody. The data represent three independent experiments.

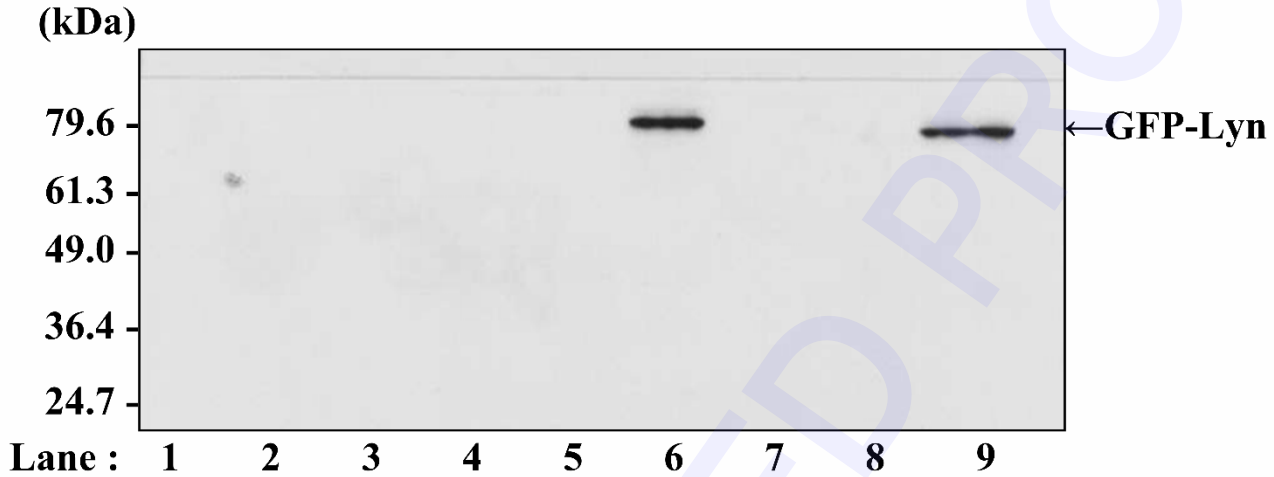

1: GST + Nor Cos1
2: GST + EGFP Cos1
3: GST + EGFP-Lyn Cos1
4: GST-rpS3 + Nor Cos1
5: GST-rpS3 + EGFP Cos1
6: GST-rpS3 + EGFP-Lyn Cos1
7: GST-rpS3C + Nor Cos1
8: GST-rpS3C + EGFP Cos1
9: GST-rpS3C + EGFP-Lyn Cos1

Supplementary Figure 2. Lyn interacts with C-terminal end of rpS3

Cos-1 cells were transiently transfected with EGFP or EGFP-Lyn. Lysates were subjected to pull down assays using 2 μg of bead bounded GST-rpS3 fusion protein, including GST-rpS3C and GST-rpS3. GST was used as the negative control. GST protein complexes were analyzed by immunoblotting with an anti-GFP antibody to detect Lyn. The data represent three independent experiments.

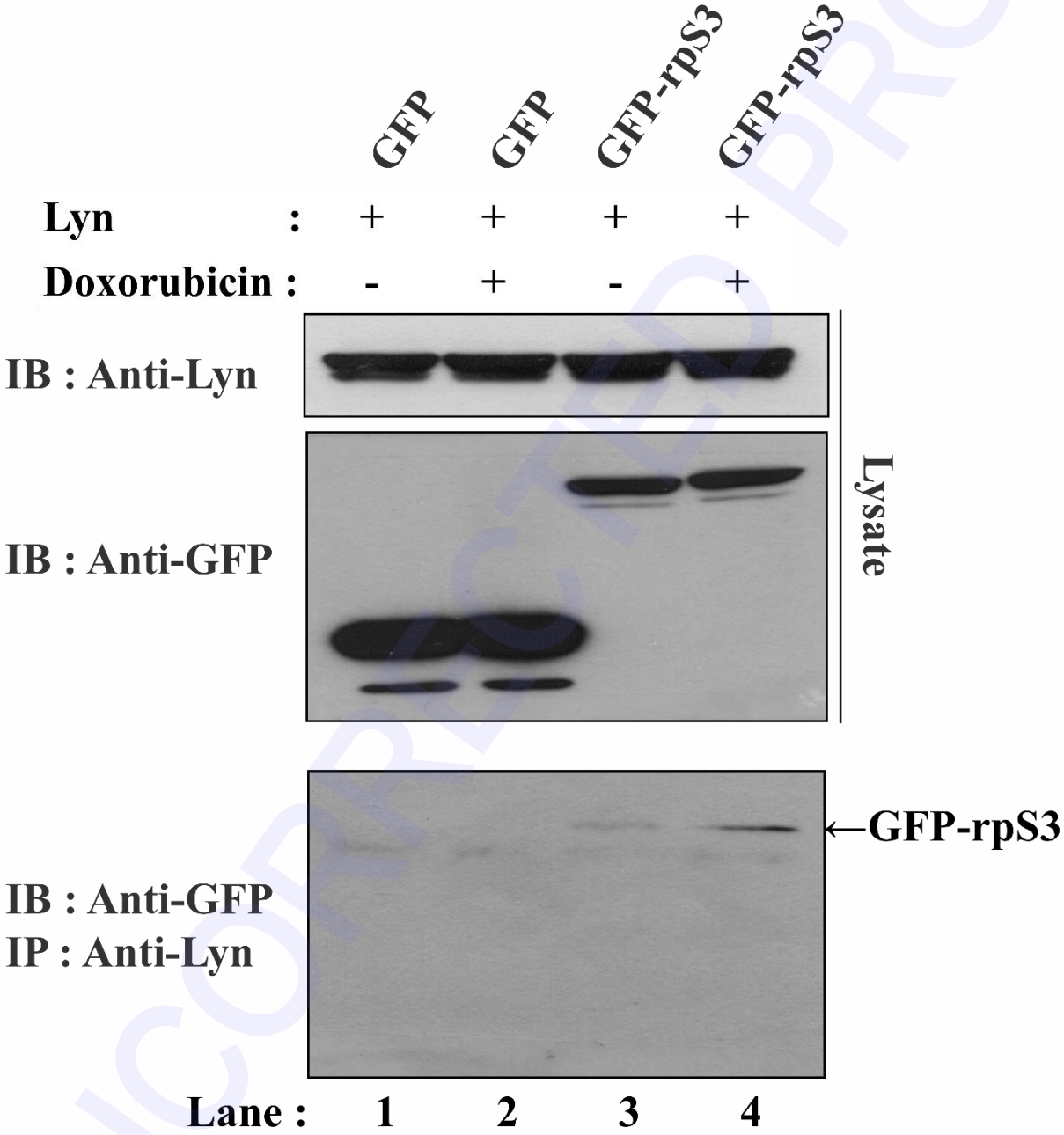

Supplementary Figure 3. Binding activity of rpS3 to Lyn is increased by the addition of doxorubicin

HEK293T cells were co-transfected with pcDNA3-Lyn and pEGFPc1 (*lanes* 1 and 2) or pcDNA3-Lyn and pEGFPc1-rpS3 plasmids (*lanes* 3 and 4), and the co-transfectants were then exposed to 1.5 μg of adriamycin (doxorubicin) for 3 h (*lanes* 2 and 4), and extracts were immunoprecipitated (IP) with Lyn antibody. Cell extracts were resolved by 10% Sodium Dodecyl Sulfate - PolyAcrylamide Gel Electrophoresis (SDS-PAGE) and immunoblotted with anti-Lyn (*upper panel*) and anti-GFP (*middle panel*) antibodies. Precipitated proteins were immunoprecipitated with Lyn antibody, resolved by 10% Sodium Dodecyl Sulfate – PolyAcrylamide Gel Electrophoresis (SDS-PAGE), and analyzed by immunoblotting (IB) with anti-GFP antibody (*upper panel*). Equal amounts of proteins were used for immunoprecipitation (IP). The data represent three independent experiments.

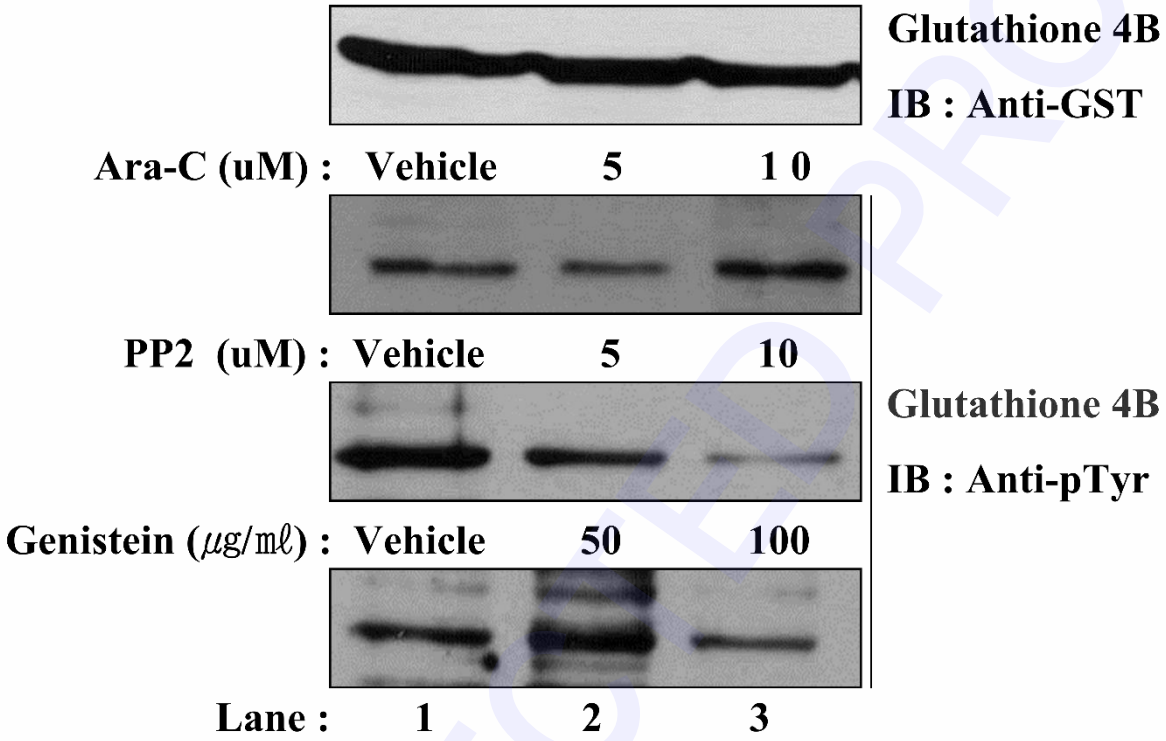

Supplementary Figure 4. Tyrosine phosphorylation of rpS3 is increased by the addition of Ara-C and is decreased by the inhibitors of tyrosine kinase

HEK293T cells were co-transfected with Lyn and GST-rpS3, and the co-transfectants were then exposed to various concentrations of drugs, including Ara-C (cytosine arabinoside, concentration 0 to 10 uM), PP2 (concentration 0 to 10 uM), and Genistein (concentration 0 to 100 μg/mL), in a dose-dependent manner for 1 h 30 min as indicated. Subsequently, the cells were treated with pervanadate. The cells

were lysed, and extracts were immunoprecipitatated (IP) with anti-rpS3 antibody. Immunoprecipitates were resolved by 10% SDS-PAGE and subjected to immunoblotting (IB) with the indicated antibodies as anti-GST and anti phospho tyrosine (pTyr) antibody. Phospho-Tyr was used to verify the effect of drug treatment. HEK293T cells treated with vehicle (Ara-C, distilled water, PP2 or Genistein; 0.1% DMSO) were used as a negative control (NC). The data represent three independent experiments.

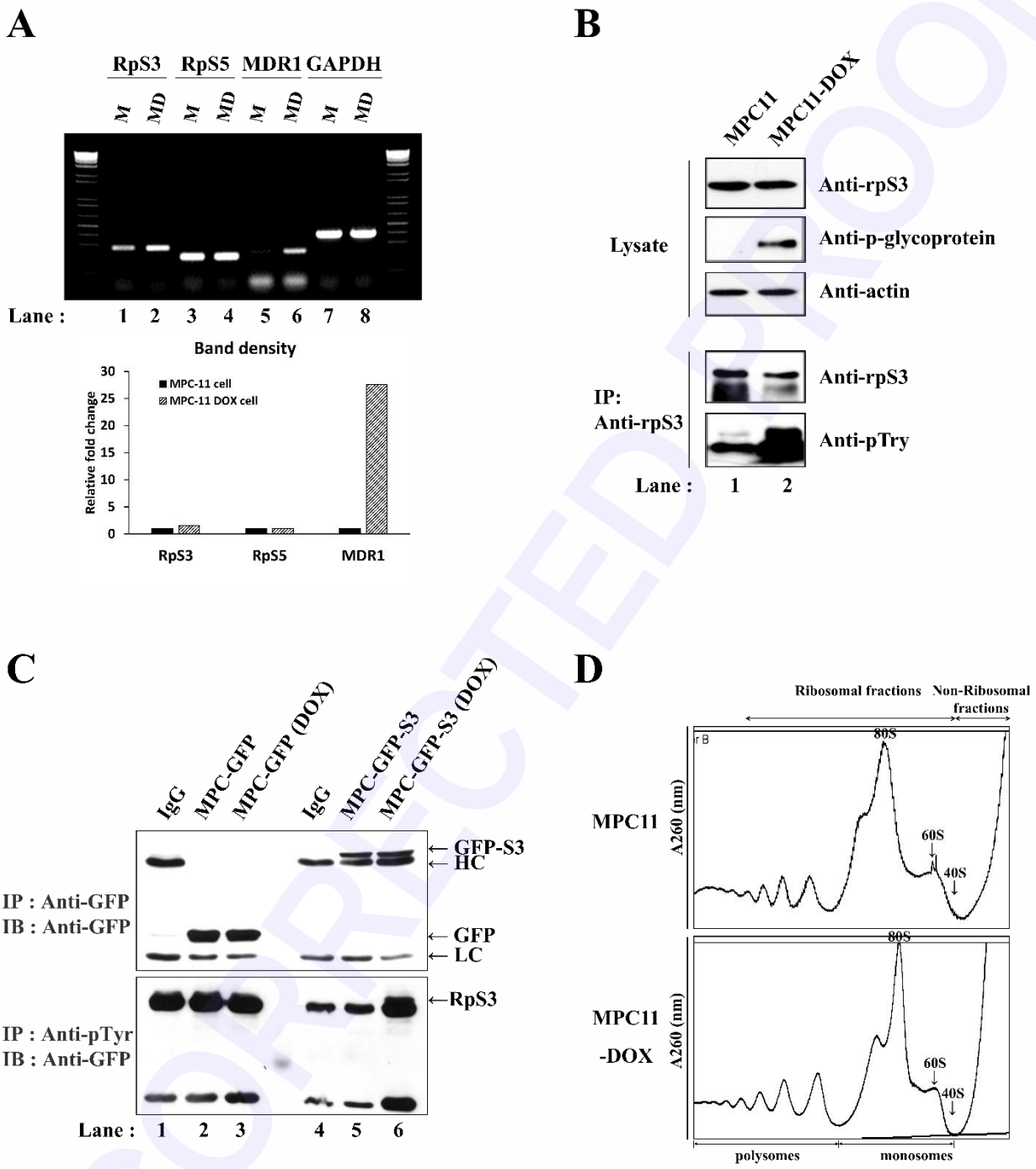

Supplementary Figure 5. Characterization of MPC11-DOX (doxorubicin 60 nM) resistant cells

(A) Comparison of expression differences of *rpS3*, *rpS5*, and *MDR1* mRNA in normal MPC-11 (M) and doxorubicin-resistant MPC-11 cells (MD) by RT-PCR analysis. Following quantitative

PCR, examination of the agarose gels confirmed that specific products of approximately 158 bp and 226 bp were obtained upon amplification of *MDR1*, *rpS3*, and *rpS5*. *GAPDH* was served as a loading control. The isolated RNAs were reverse-transcribed and amplified by PCR with *rpS3*-, *rpS5*-, *MDR1*- and *GAPDH*-specific primers. The band density of indicated genes was normalized to GAPDH (n=3). *; $p<0.05$, **; $p<0.01$ (Student's t-test). **(B)** Increased expression of p-gp and tyrosine phosphorylation of rpS3 in doxorubicin-resistant MPC-11 cell lines. Whole-cell lysates were analyzed by immunoblotting with rpS3 and p-glycoprotein antibodies in MPC-11 and MPC11-DOX cells. Immunoprecipitation assay confirmed the expression in MPC-11 and MPC11-DOX cells with the use of phospho-tyrosine antibody. Antibody to β-actin was used as a loading control. **(C)** MPC-11 cells were transfected with pcDNA3-GFP or pcDNA3-GFP-rpS3. Cell lysates (20 mg) were subjected to immunoprecipitation with anti-GFP (*upper panel*) and phospho-Tyrosine antibodies (*lower panel*), followed by immunoblot analysis with anti-GFP antibody (upper panel) and anti-phospho-tyrosine antibody (lower panel). HC; IgG heavy chain, LC; IgG light chain. **(D)** Comparison of ribosome profiles of MPC-11 and MPC11-DOX cells using ribosome profiling method using linear sucrose gradients. The polysome, monosome (80S), and ribosomal subunits (40S, 60S) regions are marked in the ribosome profile. The data represent three independent experiments.